

Double-Labeled Metabolic Maps of Memory

E. R. JOHN, Y. TANG, A. B. BRILL, R. YOUNG, K. ONO

The physical changes representing a memory are believed to be localized to specific neurons, widely distributed in multiple parallel pathways in the brain. 2-Fluorodeoxyglucose, labeled with two discriminable radioactive tracers, was used to construct quantitative metabolic maps in split-brain cats during a visual task. One side of the brain served to estimate the metabolic variability of nonspecific influences. The other side was used to map metabolic changes related to the presence of previously learned visual cues, as well as changes related to nonspecific influences, in the same periods of time. When the two sides were compared, between 5 million and 100 million neurons (depending upon the significance level selected) were identified in which activity increased during presentation of the familiar cues. The wide distribution of these neurons throughout the brain is compatible with prior evidence of a distributed memory system. However, the large number of neurons involved is difficult to reconcile with theories in which individual neurons are dedicated to specific memories.

MOST CURRENT THEORIES OF MEMORY PROPOSE THAT learning depends upon either the formation of novel connections between neurons or the alteration of efficacy of transmission along preconnected neural pathways (1-3). In microelectrode studies, plastic neurons have been found in more than a dozen brain regions, including neocortex, thalamus, hypothalamus, mesencephalon, reticular formation, amygdala, cingulate cortex, entorhinal cortex, and hippocampus (1, 4-6).

The ¹⁴C-labeled 2-deoxyglucose (2DG) method permits the assessment of local glucose utilization simultaneously in all regions of the brain (7). It is generally believed that deoxyglucose-6-phosphate cannot be fully metabolized because of its altered structure and is thus metabolically trapped inside the cell, providing a tracer for localized glucose uptake (7, 8), although there remains some disagreement as to the actual efficacy of the presumed trapping (9). This method has shown changes in regional glucose utilization in studies of the structure and physiological organization of neuro-anatomical systems mediating vision (10-14), hearing (15, 16), movement (17, 18), and activation of the limbic system (19, 20), frontal lobe neglect (21), aftereffects of brain lesions (22), drug effects (23), the metabolic activity of brain tumors (24), and the uptake of radiolabeled drugs (25). Potentially, autoradiographic (ARG) determination of the distribution of radioactively labeled 2DG utilization may provide a comprehensive map of the neural structures activated during the performance of any function by the brain. Whether the ARG's are examined qualitatively or by quantitative microdensitometry, or "QARG" (25-28), the amount of information provided is enormous.

Some studies represent an attempt to distinguish neural activity

related to a specific function from that related to nonspecific factors by comparing 2DG uptake between regions expected to mediate and those not expected to mediate the relevant function. Attention is restricted to regions selected on the basis of preconceptions about functional mediation, which may lead to failure to detect other involved regions. Tonic activating influences or unsuspected projections may produce labeling that is very difficult to evaluate [for example, see (11)]. In other studies, the average uptake of different brain regions in an experimental group is compared to the average uptake of one or more control groups. This approach depends upon the comprehensiveness and accuracy of the sampling of anatomical regions among animals and the variance of uptake within the same region among animals in the same group. The variation in uptake in such studies is difficult to evaluate. Numerous studies publish only group mean values without data about standard deviations. Some studies report standard errors or deviations that are remarkably small, while others report large standard deviations or a wide range of observed values. Many QARG studies provide no statistical evaluation of the data.

It is also difficult to precisely duplicate all the nonspecific influences acting upon the experimental group in the control group (19, 23, 29-31). The separation of uptake that is due to nonspecific influences from that specific to a particular brain function becomes of crucial importance when one examines the functional maps yielded by 2DG ARG, which characteristically reveal widespread changes in neural activity (13, 15, 17, 19, 21, 23). Thus, reports of widespread neural mediation of discrete functions could reflect inadequate control of nonspecific influences instead of mediation of various functions by a diffuse, anatomically distributed network of neurons (17, 21).

The purpose of our study was to obtain a quantitative metabolic map of the neurons mediating a specific memory, after having precisely accounted for the contribution of nonspecific influences. We used double labeling of 2-fluorodeoxyglucose with two discriminable radioactive tracers and subsequent quantitative microdensitometric analysis of serial autoradiographs to compare regional metabolic activity on two separate occasions. We devised a split-brain cat preparation that allowed metabolic variability due to nonspecific influences to be assessed on one control side of the brain during two uptake periods (each with a different radioactive tracer). The other experimental side was used to quantify uptake differences between the presence of learned cues in one uptake period versus the absence of such cues in the second uptake period. Differently colored contact lenses and transparent cues activated the control side with task-irrelevant visual input in both uptake periods and the

E. R. John is director of the Brain Research Laboratory and a professor in the Department of Psychiatry, New York University Medical Center, New York, NY 10016, and a senior research scientist at the Nathan S. Kline Psychiatric Research Institute, Orangeburg, NY 10962. Y. Tang is a visiting fellow in and A. B. Brill is chairman of the Department of Nuclear Medicine, Brookhaven National Laboratory, Upton, NY 11973. R. Young is a professor in and acting head of the Department of Physiology, University of West Indies, Kingston, Jamaica. K. Ono is an assistant professor in the Department of Physiology, Nagasaki University School of Medicine, Nagasaki 852, Japan.

experimental side with task-relevant cues in one uptake period but task-irrelevant cues in the second uptake period. Confidence levels obtained from the test-retest variability of the control side were used to estimate the statistical significance of uptake differences in the presence versus the absence of learned cues on the experimental side.

Experimental design. The design of this study overcomes the shortcomings limiting the interpretation and comprehensiveness of maps generated by QARG; our technique therefore may be applicable beyond the example of our study. Our QARG study of cerebral glucose utilization as a marker for neural activity specifically related to memory satisfied several criteria:

1) Each animal served as its own control for nonspecific influences on 2DG uptake. This was accomplished by a sequential double-label strategy (32) that controlled for inherent interregional variability within each animal. 2DG can be labeled with a variety of radioactive tracers without changing its molecular structure. It is possible to select two such tracers that differ sufficiently in half-life or energy of the emitted radiation, so that the distribution of each tracer alone can be visualized.

Two recent studies provide quantitative validation of the 2DG double-labeling strategy. In one study, unilateral multimodal stimulation was delivered to one side of the brain after [^{14}C]2DG injection, followed by stimulation of the opposite side after [^3H]2DG. Quantitative difference imaging (see below) was used to separate [^{14}C]2DG and [^3H]2DG uptake and revealed structures with high [^{14}C]2DG uptake on one side and high [^3H]2DG uptake on the other side (33). A second study (34) showed that the double-label method confirmed the selective block of anesthetic suppression of brain metabolism by a striatal lesion. In this study, a differential absorption technique was used to obtain the [^{14}C] and [^3H] images.

In order for the results of sequential double-labeling to be unambiguous, metabolism of brain regions in the control and experimental conditions must vary solely because of specific experimental influences and not because of fluctuations in nonspecific activity between the two conditions. This can only be ensured by measurement of test-retest variability in regional glucose metabolism under unchanged conditions. This requirement was difficult to satisfy, since our goal was to compare two different conditions. The double-label method by itself does not provide adequate control for nonspecific contributions to regional metabolism under such circumstances.

2) Specific information input was unequivocally lateralized. The two hemispheres of the brain can be separated in cats by the method of Sperry, which restricts the visual input to each hemisphere to that provided by the ipsilateral eye (35). In such cats, with the cerebral commissures and optic chiasm transected, visual information delivered only to one eye remains localized within the corresponding hemisphere (36). By using these split-brain cats for functional mapping studies with double-labeled 2DG, we could ascertain the variance in metabolism between different brain regions within the same condition due to inherent regional differences and also correct for the variance within the same brain regions between conditions due to changes in nonspecific influences, within the same animal.

One side of the brain served as a reference to estimate test-retest variability in uptake of 2DG due to nonspecific factors, during two successive time periods in which learned cues were not available to that side. Those data provided the baseline needed to estimate nonspecific contributions to differences found on the experimental side, comparing uptake during the first experimental period in which learned cues were available to uptake in the second control period when those cues were absent. This overall design provided sufficient information about specific and nonspecific sources of variance to permit evaluation of data from a single animal without ambiguity, and eliminated the problem caused by inherent metabol-

ic differences within the same region when separate control and experimental animals must be compared.

3) The identification of neural regions mediating the learned task was based upon comprehensive statistical evaluations rather than a priori assumptions as to the anatomical structures involved. In quantitative electroencephalographic (EEG) studies, the Z transformation of extracted features relative to the mean and standard deviation (SD) of a set of reference features detects meaningful information in a large volume of quantitative measurements (37). [$Z = (\text{individual pixel difference minus mean pixel difference})/\text{SD of the mean difference}$]. In view of the enormous amount of data generated by serial QARG, we used an analogous method. The differences in metabolic activity within each quantified neural region (pixel) between the two experimental conditions were Z-transformed against the mean and SD of the total number of difference pixels in the whole brain. The probability that the difference between neural activity in the two conditions was significant was color coded for each pixel. These data were used to generate color-coded maps (28) of significant differences in neural activity related to a specific memory, yielding a comprehensive functional map involving no a priori assumptions about the anatomical system mediating memory and learning.

Three young, mature split-brain cats were prepared by transection of the cerebral commissural tracts and the optic chiasm with the methods described by Majkowski (36). After 4 weeks, each cat was trained to obtain food in a Yerkes box consisting of a starting chamber and a runway 1 meter long, ending in two doors. There was a transparent transilluminated geometric figure on each door, two concentric circles (the positive cue) or a star (the negative cue). The areas of the positive and negative cues were equal and the side of the cues on the two doors was randomized according to a Gellerman schedule (38).

After reaching criterion (90 percent correct discrimination), each cat was trained for another 6 weeks and was then subjected to three tests. First, sessions were run with an opaque contact lens on one eye at a time. Next, the clear transparent cues were replaced by transparent green cue figures. The opaque lens was placed over one eye and a green lens over the other eye. Thus we could test each hemisphere to establish whether it could see the green cue figure. In each cat, after a brief initial period of hesitation, the discriminations were performed at criterion level with each eye. In the third test, the opaque lens was placed over one eye and a red lens over the other. Under this condition, each cat performed randomly, no matter which eye carried the red lens. We concluded that each hemisphere contained an adequate memory trace for the discrimination task, that the green lens permitted the transilluminated green cue information to be perceived, and that the red lens effectively blocked reception of green cue information.

For the 2DG experiment (39), the green contact lens was placed over one eye and the red contact lens over the other eye. In cats 1 and 2, the green lens was on the right eye and in cat 3 on the left eye. New cue cards were used, each bearing a transparent red triangle, in addition to the transparent green circles or star. Input about the learned cues (green) was thus delivered to the experimental hemisphere, while the reference side received only novel input (red) (Fig. 1). The areas of all stimuli were equal.

As soon as the contact lenses were inserted at the usually scheduled time, the cat received an intravenous injection of 100 μCi of ^{14}C -labeled 2-fluorodeoxyglucose ([^{14}C]2FDG) in one forepaw and the cat performed 60 trials (one per minute with the usual randomized schedule). During this initial uptake period, each cat performed at the criterion level or better and received approximately one half the usual amount of food per trial. After 45 minutes, most of the circulating 2FDG had been taken up from the blood. After a

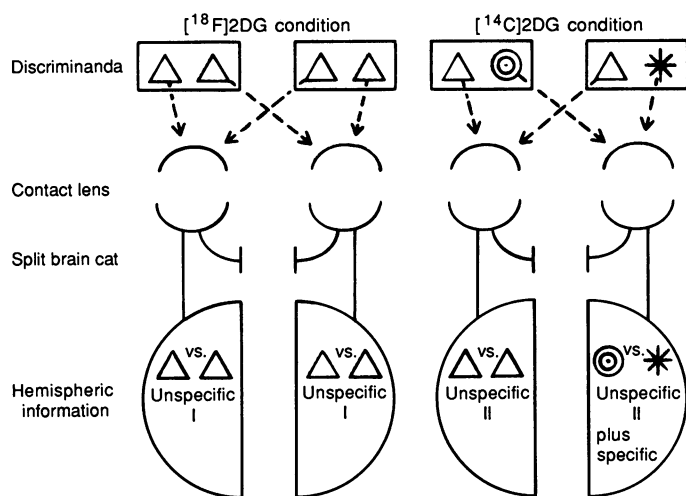


Fig. 1. Diagram of the experimental design showing information input to the cerebral hemispheres during $[^{18}\text{F}]2\text{DG}$ uptake (image I) (left) and $[^{14}\text{C}]2\text{DG}$ uptake (image II) (right). The cat was fitted with a green contact lens on the right eye.

1-hour interval, a second trial series was initiated with new cue cards, each bearing a transparent green triangle and a transparent red triangle. The red and green contact lenses remained in place. No learned cue information was now available to either hemisphere (40). At the beginning of this series, the cat received an injection of 20 to 30 μCi of ^{18}F -labeled 2-fluorodeoxyglucose ($[^{18}\text{F}]2\text{FDG}$) in the other forepaw. The cat then performed 60 trials at one per minute. During this second uptake period, each cat performed at the random level, dividing its decisions almost equally between the two sides and displaying only temporary hesitation. All choices were reinforced with food, approximately one half the usual amount. Each cat ran exactly the same distance in the same amount of time as under the previous condition and received the same amount of food.

As soon as the second uptake period was completed, each cat was killed by an intravenous injection of a pentobarbital excess. The cat was perfused with 10 percent Formalin, the brain was removed, frozen in an alcohol bath containing liquid CO_2 , and imbedded in carboxymethyl cellulose. Serial horizontal sections 30 μm thick were made with a whole body cryomicrotome (LKB). Alternate sections were air-dried and placed on mammography film at -70°C for ARG's. Every tenth section was selected for conventional histologi-

cal staining. Commercially prepared ^{14}C standards (41) and various activities of ^{18}F were used for standardization. After 8 hours the film was removed, yielding image I (Fig. 1, left). Twelve hours later when the ^{18}F activity had decayed to less than 0.1 percent of its initial value, the sections were again placed on mammography film. Fifteen days later, the film was removed, yielding image II (Fig. 1, right) (42). The methods and systems used in these studies are presented in greater detail elsewhere (25, 26, 43).

The conditions governing $[^{14}\text{C}]2\text{DG}$ uptake in the first session are shown in Fig. 1, right, for a cat with the green lens on the right and the red lens on the left eye. Both sides of the brain were subject to the same nonspecific influences, but the right side received input from learned green cues and the left side received input from red patterns with no cue value. The conditions governing $[^{18}\text{F}]2\text{DG}$ uptake in the second session are shown on the left side of Fig. 1 for the same cat. Both sides of the brain were again subject to the same nonspecific influences, but now both the green and red patterns had no cue value.

Because the half-life of ^{18}F is very short relative to that of ^{14}C , the first autoradiograph primarily reflected the rapid decay of ^{18}F taken up during the informationally symmetric conditions of the second session. However, due to the presence of the ^{14}C taken up during the informationally asymmetric conditions of the first session, the two sides of this autoradiograph were differentially contaminated by the slow decay of ^{14}C , or ^{14}C "shine". This ARG is referred to as image I. The second ARG, taken after the decay of ^{18}F in the brain sections was essentially complete, reflected only uptake during the informationally asymmetric first session, and is referred to as image II.

Image processing. The image processing procedure was designed (i) to quantify the regional 2DG uptake on the reference and experimental sides of the two images obtained from each brain section (quantification), (ii) to align the two images (registration), (iii) to remove the ^{14}C shine (purification), (iv) to correct for the difference in capture efficiency of the photographic emulsion for the different energies of the two tracers (conversion), (v) to compensate for differences in the specific activity of the glucose pool for the two tracers (normalization), (vi) to subtract image I from image II (subtraction), and (vii) to scale the resulting difference image in a statistically interpretable manner (Z transformation). On the reference side, this procedure yields an image of regional test-retest metabolic variability, that is, metabolic noise. On the experimental side, this image reflects activity associated with regional mediation of memory plus metabolic noise. Appropriate scaling of the differ-

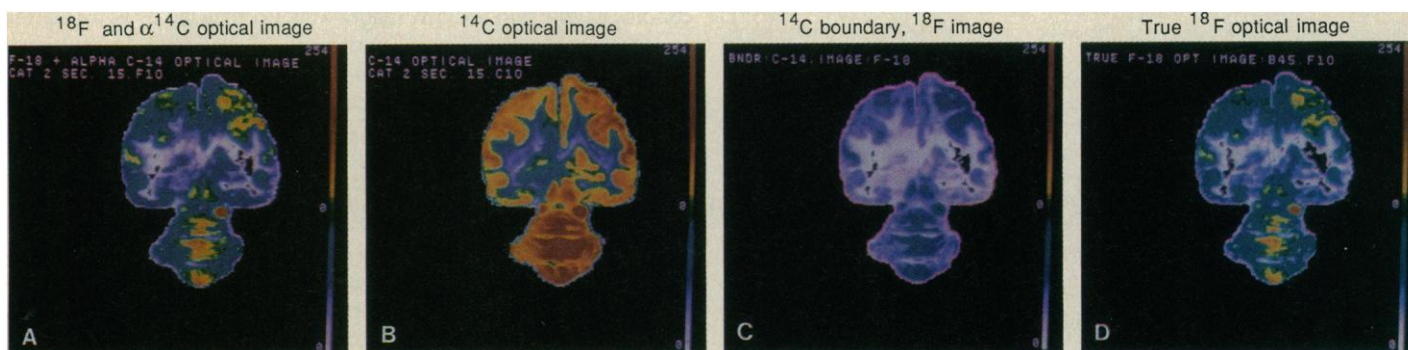


Fig. 2. Computer-generated images of the same brain section (15.10) during sequential stages in processing. The color coding on these images is a "heat" scale ranging from white to red as the optical density increases. The color scale to the right of each image confirms reproducibility of the palette used for color coding of densitometric data. (A) Optical density image I, showing distribution of $[^{18}\text{F}]2\text{DG}$ uptake contaminated by $[^{14}\text{C}]2\text{DG}$ also present in

the tissue. $\alpha = T1/T2$, where T1 is time of film exposure to $[^{18}\text{F}]2\text{DG}$ and T2 is time of film exposure to $[^{14}\text{C}]2\text{DG}$. (B) Optical density image II showing distribution of $[^{14}\text{C}]2\text{DG}$. (C) Boundary of image II (pink line) encircles pale blue image I after registration of the two images. (D) True $[^{18}\text{F}]2\text{DG}$ optical image after subtraction of an amount of image II proportional to the exposure ratio α .

Z transformation was then needed because the significances of the differences between the two test conditions in Fig. 3E are difficult to evaluate because the color scale is in microcuries. For the difference in any local region to be interpretable as the metabolic consequences of activation of a specific memory, rather than random metabolic fluctuations or noise, the noise variance must be taken into consideration. To accomplish this, we computed the mean value and SD of all pixels on the control side from the difference image, for each section separately. These statistics were then used to Z-transform each pixel in the difference image. We then computed the Z-transformed difference image (Fig. 3F). The color scale for the Z image directly reflects the probability that the difference in glucose utilization observed in any pixel arises from random metabolic variance or from participation (excitatory or inhibitory) in the activation of a specific memory.

Comparison of the optical image (Fig. 3A) and the Z-transformed difference image (Fig. 3F) shows that the anatomical distribution of regions participating in a specific memory (Fig. 3F) is different from that suggested by Fig. 3A. This indicates the extent to which nonspecific influences may lead to misleading results in 2DG functional mapping with only a single label.

Alternative image processing procedures. Despite the clarity of results yielded by the image processing methods just described, a number of alternative approaches might have been used. We evaluated all of these alternatives.

The first of these was ratio images. Normalization was accomplished by equating the total metabolic activity of the reference side between the two images, separately for each section. Although this accomplished normalization in the absolute statistical sense, the relative effect on individual regions with different levels of activity was not the same, which might yield misleading results. One way to circumvent this difficulty and to eliminate the need to construct a difference image, is to compare metabolic activity in the two conditions by computing the ratio activity II/activity I for each pixel. If such data were evaluated relative to the average ratio, this would effectively constitute normalization.

Relative differences could also be calculated. An absolute difference image was constructed by subtraction of image I from image II. The same absolute difference value might be found for two regions that differed greatly in their metabolic activity. For a region with very high activity, a given difference value might represent a negligible change in metabolic activity, while for a region with low activity, the same value might represent a very marked change. This difficulty can be circumvented by computing the relative (percent) difference image; that is, $(\text{image II} - \text{image I}) / \frac{1}{2} (\text{image II} + \text{image I})$.

Z transformations were computed relative to the mean value and SD of the distribution of difference values for both absolute and relative differences, as well as for ratio values, across all pixels on the reference side of each section. This introduced a possible bias toward positive findings because random effects could be expected to impose a somewhat different distribution on the experimental side of that section. This bias might be minimized by using the mean and SD of all pixels in each individual whole section since the expected variance would be larger. However, the range of average values and metabolic activity might vary appreciably between different levels of the brain. The same Z value, obtained for two difference pixels transformed relative to the distributions of activity at two different levels, might reflect extremely different metabolic effects. This possibility could be minimized by the use of the mean and SD of all pixels in the entire reference hemisphere. This introduces the same possibility of positive bias, across the full set of sections, as was introduced by the use of the reference side of each section as the standard. The obvious solution to this problem would be to use the

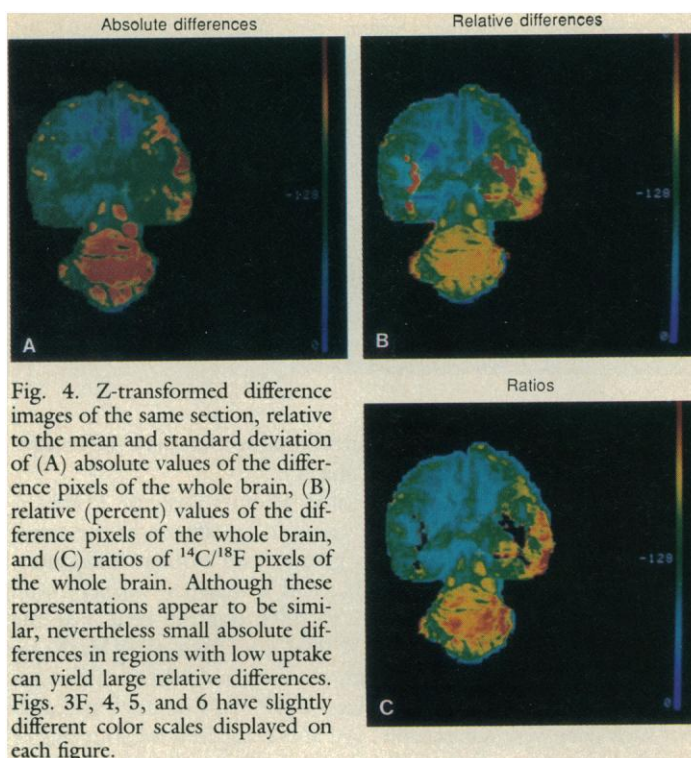


Fig. 4. Z-transformed difference images of the same section, relative to the mean and standard deviation of (A) absolute values of the difference pixels of the whole brain, (B) relative (percent) values of the difference pixels of the whole brain, and (C) ratios of $^{14}\text{C}/^{18}\text{F}$ pixels of the whole brain. Although these representations appear to be similar, nevertheless small absolute differences in regions with low uptake can yield large relative differences. Figs. 3F, 4, 5, and 6 have slightly different color scales displayed on each figure.

mean and SD of all pixels in the whole brain. This introduces the possibility of obscuring important details because the metabolic variance across the whole brain can be expected to be enormous.

These alternative approaches to image processing were analyzed by comparing the distributions of pixel values of the two sides of the split brain for absolute differences, relative differences, and ratios between the two images. We used Z transformations against the mean and SD of the pixel distributions in the whole brain, the whole

Table 1. Difference between Z-transformed pixel distributions in information and reference hemispheres. Data are expressed as information minus reference.

Z transformation reference	Absolute differences	Relative (%) differences	Ratios
Whole brain			
Mean	0.1149	0.1005	0.0459
SD	-0.0026	0.0138	0.0935
% above mean	5.18	4.44	1.74
% above 1.96 SD	0.35	0.38	0.37
% above 2.56 SD	0.23	0.20	0.31
Whole reference hemisphere			
Mean	0.1149	0.1015	0.0482
SD	-0.0027	0.0138	0.0982
% above mean	5.18	4.54	1.80
% above 1.96 SD	0.36	0.41	0.30
% above 2.56 SD	0.23	0.22	0.34
Each whole section			
Mean	0.1186	0.0962	0.0844
SD	-0.0122	-0.0107	0.0530
% above mean	5.29	4.18	3.92
% above 1.96 SD	0.29	0.22	0.29
% above 2.56 SD	0.15	0.15	0.14
Reference side each Section			
Mean	0.1219	0.1009	0.1003
SD	0.0154	0.0133	0.1258
% above mean	5.19	4.43	4.12
% above 1.96 SD	0.75	0.29	0.63
% above 2.56 SD	0.38	0.18	0.28

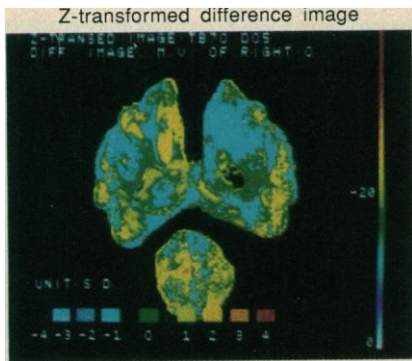


Fig. 5. Z-transformed difference image from cat 3, with left information side. This section is at Horsley-Clarke (Hc) plane + 9.2 mm. The color scale is in units of SD around the mean for the whole brain. Compare to Fig. 6, panel 7, the corresponding section from cat 2, with right information side.

control hemisphere, each whole individual section, and the control side of each individual section (Table 1).

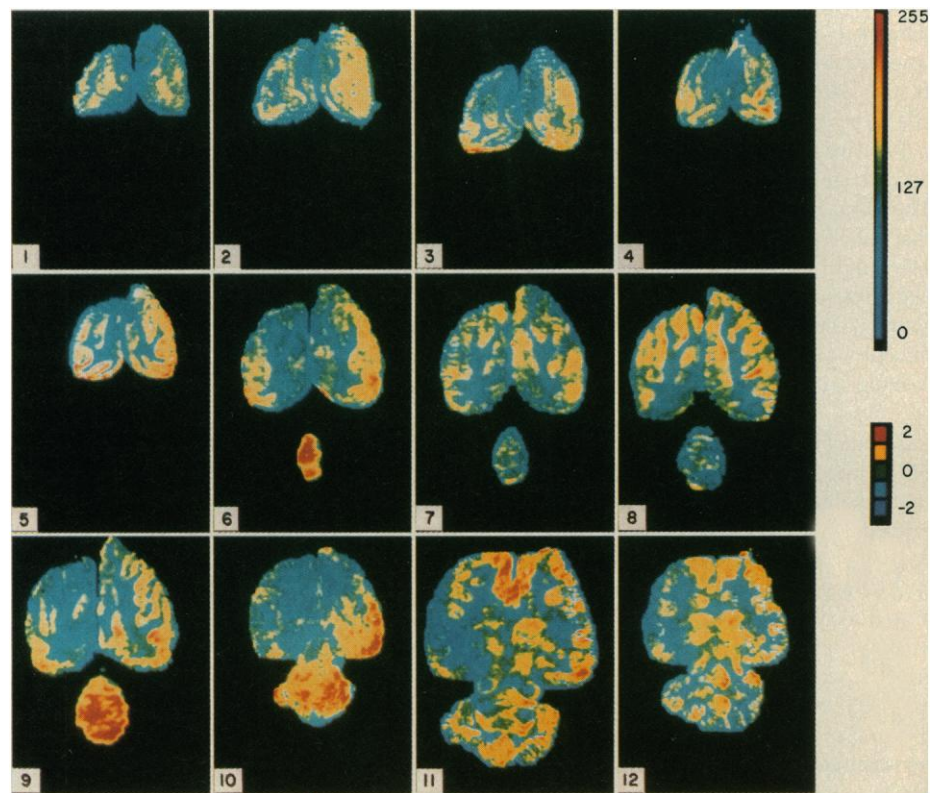
The results are essentially the same whether absolute (Table 1, column 1) or relative (Table 1, column 2) differences are used, although the differences tend to be greater with absolute differences. Ratio data (Table 1, column 3) yield somewhat smaller mean differences and larger differences in SD's but the results at the $P < 0.05$ ($>1.96 \times \text{SD}$) and $P < 0.01$ ($>2.56 \times \text{SD}$) levels are comparable to those obtained with absolute and relative difference measures. The larger SD differences of the ratio method indicated that such data were less reliable. We also compared the four sets of statistical parameters that could be used for Z transformation (Table 1). The results obtained with Z transformation with any of the four reference distributions were similar, with a few exceptions. All 12 approaches supported the same qualitative conclusion and Z transfor-

mation yielded similar images for these different treatments of the data (Fig. 4). Thus, Z transformations of the distributions of metabolic activity in double-label studies converge to an approximately canonical or "true" description, regardless of which approach is used for initial extraction of descriptive features or reference statistics.

Neural activity associated with the memory task. A typical Z-transformed difference image from cat 3 is shown in Fig. 5. The asymmetry is evident, with the information side (left) displaying greater differences between the two uptake periods than the reference side, indicating that the metabolism of some regions on the left during the processing of the learned cues (first uptake period) was significantly greater than when processing novel input (second uptake period). The yellow (2 SD's above the mean, $P < 0.05$), orange (3 SD's above the mean), and red (4 SD's above the mean) indicate significant differences. The asymmetries are most marked in the cingulate gyrus, caudate nucleus, and vermis of the cerebellum. The control side displays little or no differences above the 0.05 level. This image is similar to that obtained at the corresponding brain level from cat 2 (Fig. 6, panel 7), with reversal of the information side (on the right for cat 2).

We computed the difference between the information and reference hemispheres using the distributions of absolute differences in metabolic activity between image I and image II in two maps, Z-transformed relative to the pixel distribution of the whole brain (most conservative) as well as relative to the reference side of each section (least conservative) (Table 2). The steps in image processing illustrated in Figs. 2 and 3 were applied to horizontal sections selected at about 0.75-mm intervals from the top to the bottom of the brains (46). In cats 1 and 2, in which the experimental side was

Fig. 6. Z-transformed difference images of cat 2 from just below the dorsal surface of the brain to just above the ventral margin of the split, relative to the mean and SD of the absolute difference of all pixels in the whole brain. The color scale is in units of SD around the mean for the whole brain. Identification of asymmetrical regions selectively involved in mediation of memory was made with the histologically stained sections prepared from every tenth slice, in conjunction with the horizontal atlas of the cat brain published by Berman (46). Numerous anatomical regions in this figure display marked asymmetry as follows. (panel 1) Section 3.12 (Hc = 13.8), posterior suprasylvian gyrus; (panel 2) section 4.07 (Hc = 13.4), medial suprasylvian gyrus, posterior suprasylvian gyrus, medial ectosylvian gyrus, posterior lateral gyrus; (panel 3) section 5.07 (Hc = 12.7), medial suprasylvian gyrus, posterior suprasylvian gyrus, medial ectosylvian gyrus, posterior lateral gyrus; (panel 4) section 6.12 (Hc = 11.7), anterior lateral gyrus, medial suprasylvian gyrus, posterior lateral gyrus; (panel 5) section 7.06 (Hc = 11.1), anterior lateral gyrus, medial suprasylvian gyrus, medial ectosylvian gyrus; (panel 6) section 8.12 (Hc = 10.1), anterior suprasylvian gyrus, posterior suprasylvian gyrus, medial ectosylvian gyrus, posterior lateral gyrus, cingulate gyrus; (panel 7) section 9.12 (Hc = 9.3), posterior suprasylvian gyrus, anterior lateral gyrus, cingulate gyrus, caudate nucleus, vermis of cerebellum; (panel 8) section 10.10 (Hc = 8.7), posterior suprasylvian gyrus; cingulate gyrus, vermis; (panel 9) section 11.07 (Hc = 8.2), anterior lateral gyrus, anterior suprasylvian gyrus, anterior ectosylvian gyrus, posterior suprasylvian gyrus, anterior ectosylvian gyrus, posterior suprasylvian gyrus, cingulate gyrus, dorsal hippocampus, vermis; (panel 10) section 15.10 (Hc = 5.1), posterior ectosylvian gyrus, posterior lateral gyrus, vermis, crus I of



cerebellum, pulvinar, lamina medullaris, posterior dorsal thalamic nuclei, hippocampus, periaqueductal gray, superior colliculus; (panel 11) section 18.11 (Hc = 2.9), anterior lateral gyrus, posterior lateral gyrus, vermis, crus I, red nucleus, paraventricular nucleus, superior colliculus, medial

pretectal area, mediadorsal thalamic nucleus, central lateral nucleus, subiculum; (panel 12) section 21.10 (Hc = 0.8), anterior lateral gyrus, medial geniculate, vermis, crus I, nucleus interpositus, medial cerebellar nucleus, parafascicular nucleus, ventromedial thalamic complex.

on the right, consistently greater differences between the experimental and control conditions were seen on the right side. The brain of cat 1 was warped during freezing and was not suitable for quantitative analyses, but showed qualitative asymmetries like those seen in cat 2. In cat 3, for which the experimental side was on the left, the converse was true.

Z-transformed difference images are shown from cat 2, at intervals from the surface of the brain to a level just above the ventral margin of the surgical separation of the two sides ($H_c = +0.50$) (Fig. 6). These Z-transformed images are based upon the mean and SD of the distribution of difference pixels in the whole brain. The neural activity, reflected by local cerebral glucose utilization, was significantly higher in most sections on the right side in the [^{14}C]2FDG uptake period, when learned shapes were perceived by the right side and novel shapes perceived by the left, than in the [^{18}F]2FDG uptake period, when both sides perceived novel shapes with no cue value. Many anatomical regions on the right side displayed significantly greater neural activity when a specific memory was activated. These included most cortical areas, much of the limbic system, the thalamus, and the cerebellum. Although neural activity was widespread, some regions seemed more active than others, in particular the anterior and posterior lateral gyrus, the medial and posterior suprasylvian gyrus, the medial ectosylvian gyrus, the cingulate gyrus, the superior colliculus, the hippocampus, and the vermis.

The probabilistic color coding of images 6.1 to 6.4 shows a maximum cortical asymmetry in the region from 2.6 to 3.3 mm below the top of the brain. Because the brain surface is slightly concave, with respect to the highest point on the midline, this suggests activity of cortical cells in layer 4, which lies about 1.4 mm below the surface. This asymmetry was obvious through Fig. 6, panel 12 which lies just above the ventral margin of the split-brain preparation. Sections below this level tended to be more symmetrical but may be involved in memory.

The distributions of values in the difference pixels, whether Z-transformed relative to each separate section, the reference hemisphere, or to the brain as a whole were only slightly different. For both cases, the mean value was essentially zero and the SD was 1.00. The histogram of Z values for each section systematically showed a greater range relative to the whole brain than relative to the section itself, indicating that significant differences did exist in the absolute level of metabolism at different H_c levels. These differences, however, were usually due to a small proportion of the cells in any section, which represented the extremes of activation or inhibition. Although such differences could be demonstrated by quantitative comparison, they were hard to discern by simple visual inspection of the difference image of the same section Z-transformed relative to the different distributions. (For example, compare Fig. 3F, cat 2, section 15.10, Z-transformed with respect to its reference side with Fig. 6, panel 10, the same section Z-transformed with respect to the whole brain.) For each section, the distribution of pixels in the Z-transformed difference image was computed separately for the reference and the experimental sides.

Of the 53 sections sampled in the two cats, 47 had a greater percentage of difference pixels above the mean value on the experimental side than the reference side. This event has a probability of 0.29×10^{-8} (47). At the $P < 0.05$ level, 31 sections out of 53 had a greater percentage of difference pixels above the mean value on the experimental side than the reference side (not significantly different). At the $P < 0.01$ level, 35 sections out of 53 had a greater percentage significantly above the mean value on the experimental side than the reference side. The probability of this event was 0.013.

Cats 2 and 3 were slightly different in weight (3.0 and 2.4 kg).

Table 2. Experimental minus reference hemisphere differences between distributions of Z-transformed absolute difference pixels. $P \leq 0.05$ when difference is above 1.96 SD and $P \leq 0.01$ when difference is above 2.56 SD.

	Differences (%)	
	Relative to whole brain	Relative to reference side of each section
<i>Cat 2</i>		
Above mean	5.18	5.19
Above 1.96 SD	0.35	0.75
Above 2.56 SD	0.23	0.38
<i>Cat 3</i>		
Above mean	6.16	6.20
Above 1.96 SD	0.87	1.33
Above 2.56 SD	0.65	1.00

The total number of pixels in the brains of the two cats were somewhat different, with 13,854,192 for cat 2 and 11,314,728 for cat 3. If we assume that the two brains contained the same number of neurons, about 2 billion, then the average pixel contained 144 neurons in cat 2 and 177 neurons in cat 3.

Because our experimental design corrected for nonspecific differences between the two uptake conditions, all the differences in the distribution of Z values between the experimental and reference sides of the brain could be attributed to neural activity related to processing information about the learned shapes on the experimental side. More rigorous criteria might include in the memory system only neurons in those pixels for which the difference between the two uptake conditions was significant at the $P < 0.05$ level or at the $P < 0.01$ level.

In cat 2, 53.22 percent of the pixels on the experimental side, but only 48.03 percent of the pixels on the reference side, exceeded the mean of the reference side of each section. The corresponding values at the $P < 0.05$ level were, respectively, 3.54 and 2.79 percent and, for the $P < 0.01$ level, 1.09 and 0.71 percent. The corresponding values above the mean of the whole brain were 50.82 percent and 45.64 percent for the experimental and reference sides, respectively. The data at the $P < 0.05$ level were 3.00 and 2.65 percent, and at the $P < 0.01$ level, 1.08 and 0.85 percent. Similar results were obtained for cat 3 (Table 2).

It is not possible to estimate the variation in neural metabolism among the neurons within each pixel. A high difference value in a pixel might reflect lack of homogeneous participation of neurons within the sampled volume, with some proportion of the cells being greatly activated, or it might reflect generally higher metabolism characteristic of most or all neurons in the volume. Because metabolism was raised so extensively and because so many neurons show plasticity in electrophysiological studies (4-6), the latter assumption seems more probable.

The observed distributions of difference pixels, in conjunction with the estimate of neurons per pixel in each cat, indicate that in cat 2, about 104×10^6 neurons displayed increased activity, about 15×10^6 displayed an increase in activity significant at the $P < 0.05$ level, and about 7.6×10^6 an increase significant at the $P < 0.01$ level, with Z transforms relative to each separate section. If we use Z transforms relative to the whole brain, the corresponding numbers of neurons are 103×10^6 , 7×10^6 , and 4.6×10^6 .

Z transforms relative to each section indicated that for cat 3 the number of neurons showing greater than mean activation differences was 124×10^6 , with 26.6×10^6 showing differences significant at $P < 0.05$ and 20×10^6 significant at $P < 0.01$. In contrast, Z transforms relative to the whole brain indicated that the corresponding numbers of neurons were 123×10^6 , 17.4×10^6 , and

13×10^6 . These approximations fail to take into account those regions showing significant levels of inhibition of neural activity, which might further increase these estimates of the number of neurons in the representational system.

Distributed storage of memory. 2DG QARG has been used to study the anatomical distribution of neural activity related to learning or memory (29–31, 40, 44, 48, 49). The issues of experimental design and control of nonspecific influences on neural activity discussed above are particularly relevant to the attempts to construct a metabolic map of the systems involved in memory and learning, because no substantiated a priori theory exists for the systems or pathways that might be involved.

In two studies—one comparing self-stimulated to experimentally stimulated animals receiving reinforcing electrical stimulation (49) and another comparing trained, yoked controls, and resting controls in avoidance learning (29)—differences in neural activity were observed between trained animals and controls for nonspecific effects of stimulation. A widespread pattern of weak changes was seen, involving many brain structures, but it was difficult to separate specific learned effects from nonspecific effects reflecting possible differences in arousal and amount and type of movements. In another study (31) that compared uptake in resting control monkeys with uptake in monkeys performing a conditioned motor task in response to a visual stimulus to avoid shock asymmetrical differences in uptake of motor system structures were observed. These changes were related to the unilateral task performance, but widespread symmetrical activation of structures in the visual and auditory systems was also observed, presumably attributable to nonspecific effects. However, because there was a visual cue for the motor avoidance response, some of the observed changes might reflect involvement of visual system structures in the learned performance. Thus, separation of nonspecific symmetrical from task-related symmetrical activation outside the motor system was ambiguous.

In our studies, the reference side of the brain was subject to multiple nonspecific influences, reflecting such systemic variables as blood pressure, heart rate, autonomic factors, arousal, motivation, movement, novel red-patterned visual input, olfactory inputs from the experimenter and the apparatus, and the ingestion of food. The experimental side of the brain was subject to these same nonspecific influences but with learned green-patterned visual input.

In a study of neural activity in the inferior colliculus during establishment of classical aversive conditioning to a tone conditioned stimulus (CS) paired with an aversive shock to the reticular formation unconditioned stimulus (US), Gonzalez-Lima and Scheich (44) concluded that most of the tonotopic space in the frequency range of the stimulus was involved in conditioning. They pointed out that this does not necessarily mean that all neurons within that space participate, but considered as unlikely the alternative that a minority of plastic neurons was concentrated in a fraction of the conditioned tonotopic volume of cells. They suggested that sensory learning is achieved by an anatomically distributed population of cells. In contrast, in studies of imprinting (30, 48) few regions showed a significant difference between experimental and control groups. In one of these studies (30), it was noted that other differences might be obscured by the nonspecific differences in arousal states between imprinted and nonimprinted chicks and suggested that further investigations with split-brain chicks might be necessary to clarify this issue.

Many of the structures shown to mediate memory in our study have been implicated by previous ARG investigations. Further, our data are also compatible with microelectrode studies, which reveal changes in the firing patterns of plastic cells in various of these brain regions during learning (1, 4, 5) and show that high proportions of cells in such regions display plasticity (6, 50).

The assumption in current efforts to localize plastic changes with learning is that those changes occur in discrete pathways. It is further assumed that after learning, augmented neural firing in those discrete pathways represents each specific memory, no matter how redundant or anatomically distributed such firing might be. The vast number and anatomical extensiveness of the neurons here shown to participate in representation of a single and rather simple memory is hard to reconcile with these assumptions. So many neurons seem to be involved in mediation of one specific learned discrimination that there simply are not enough neurons available to represent any reasonable store of memories with this degree of redundancy. It is difficult to conceive of a plausible mechanism for decision-making that might integrate and interpret activity in so many anatomically distributed parallel circuits. Pending further research to establish the extent to which our results might reflect the operation of some general memory retrieval system, the sheer number of cells involved requires that most plastic cells participate in multiple memories. Dedicated redundant circuits or complex feature extractors, converging to specific percept or memory detectors (1, 3), do not seem plausible.

Our results also do not fit well with a general computer-like model of the brain, with information stored in discrete registers, no matter how many in number (3, 4). A radically different model is necessary. Our data, like data from diverse electrophysiological and anatomical studies reviewed elsewhere (50), better support notions of cooperative processes, in which the nonrandom behavior of huge ensembles of neural elements mediates the integration and processing of information and the retrieval of memories. In view of the large number of neurons involved, the question of how the information represented in these neurons can be evaluated and appreciated by the brain becomes of critical theoretical interest. No conceivable neuron or set of neurons, no matter how diffuse its synaptic inputs, can evaluate the enormous amount of neural activity here shown to be involved in retrieval of even a simple form discrimination. Memory and awareness in complex neural systems may depend upon presently unrecognized properties of the system as a whole, and not upon any of the elements that constitute the system.

REFERENCES AND NOTES

1. C. D. Woody, *Memory, Learning and Higher Function* (Springer-Verlag, New York, 1982).
2. I. Kupferman, in *Principles of Neural Science*, E. R. Kandel and J. H. Schwartz, Eds. (Elsevier, New York, 1985).
3. E. R. Kandel, *ibid.*
4. C. D. Woody, *Conditioning: Representation of Involved Neural Function* (Plenum, New York, 1982).
5. D. Alkon and J. Farley, Eds. *Primary Neural Substrates of Learning and Behavioral Change* (Cambridge Univ. Press, New York, 1984); J. Farley and D. Alkon, *Annu. Rev. Psychol.* **36**, 419 (1985).
6. R. F. Thompson *et al.*, *Prog. Psychobiol. Physiol. Psychol.* **10**, 167 (1983).
7. L. Sokoloff *et al.*, *J. Neurochem.* **28**, 897 (1977).
8. C. Kennedy *et al.*, *Science* **187**, 850 (1975).
9. W. Sacks, S. Sacks, A. Fleischer, *Neurochem. Res.* **8**, 661 (1983).
10. I. Diviac, *Neuroscience* **10**, 1151 (1983).
11. P. Bagnoli and W. Francesconi, *Exp. Brain Res.* **53**, 217 (1984).
12. L. C. Skeen and D. P. M. Northmore, *Neurosci. Lett.* **52**, 191 (1984).
13. K. A. Macko *et al.*, *Science* **218**, 394 (1982).
14. M. Tigges, A. E. Hendrickson, J. Tigges, *J. Comp. Neurol.* **227**, 1 (1984); W. Singer, B. Freeman, J. Rauschecker, *Exp. Brain Res.* **41**, 199 (1981); R. B. Tootell, M. S. Silverman, R. L. De Valois, *Science* **214**, 813 (1981); I. D. Thompson, M. Kossut, C. Blakemore, *Nature (London)* **301**, 712 (1983).
15. J. Serviere, W. R. Webster, M. B. Calford, *J. Comp. Neurol.* **228**, 463 (1984).
16. K. K. Glendenning, K. A. Hutson, R. J. Nudo, R. B. Masterton, *ibid.* **232**, 261 (1985).
17. S. J. Juliano, P. J. Hand, B. L. Whitsel, *J. Neurophysiol.* **50**, 961 (1983).
18. K. R. Brizzee and W. P. Dunlap, *Brain Behav. Evol.* **23**, 14 (1983).
19. M. Brurus *et al.*, *Brain Res.* **310**, 279 (1984).
20. M. Brurus, M. B. Shaikh, H. E. Siegel, *ibid.*, p. 235; R. E. Watson, Jr., H. M. Edinger, A. Siegel, *ibid.* **269**, 327 (1983).
21. R. K. Duell and R. C. Collins, *Ann. Neurol.* **15**, 521 (1984).
22. R. M. Cooper and G. A. Thurlow, *Exp. Neurol.* **86**, 261 (1984).
23. L. V. Porrino, G. Lucignani, D. Dow-Edwards, L. Sokoloff, *Brain Res.* **307**, 311 (1984).

24. R. G. Blasberg, D. Groothuis, P. Molnar, *Semin. Neurol.* **1**, 203 (1981); R. G. Blasberg *et al.*, *J. Pharmacol. Exp. Ther.* **231**, 724 (1984).
25. Y. Yonekura *et al.*, *J. Nucl. Med.* **24**, 231 (1983).
26. Y. Yonekura and A. B. Brill, in *Diagnostic Imaging in Medicine*, R. C. Reba, D. J. Goodenough, H. F. Davidson, Eds. [NATO ASI Series No. 61 (1983)].
27. C. R. Gallistel *et al.*, *Neurosci. Biobehav. Rev.* **6**, 409 (1982).
28. C. Gooch, W. Rasband, L. Sokoloff, *Ann. Neurol.* **7**, 359 (1980).
29. M. Shimada, H. Murakami, T. H. Imahayashi, H. S. Ozaki, *J. Anat.* **136**, 751 (1983).
30. S. Kohsaka, K. Takamatsu, E. Aoki, Y. Tsukada, *Brain Res.* **172**, 539 (1979).
31. R. J. Schwartzman, J. Greenberg, M. Revich, K. J. Klose, G. M. Alexander, *Exp. Neurol.* **72**, 153 (1981).
32. L. L. Altenau and B. W. Agranoff, *Brain Res.* **153**, 375 (1978); B. W. Agranoff and L. L. Altenau, *Proc. Int. Soc. Neurochem.* **6**, 513 (1977).
33. H. R. Friedman, C. J. Bruce, P. S. Goldman-Rakic, *Soc. Neurosci. Abstr.* **10**, 1002 (1984).
34. J. L. Olds, K. A. Frey, R. L. Ehrenkauf, J. Patoki, B. Agranoff, *Soc. Neurosci. Abstr.* **10**, 1002 (1985).
35. R. W. Sperry, in *Interhemispheric Relations and Cerebral Dominance*, V. B. Mountcastle, Ed. (Johns Hopkins Univ. Press, Baltimore, 1962).
36. J. Majkowski, *Electroencephalogr. Clin. Neurophysiol.* **23**, 521 (1967).
37. E. R. John *et al.*, *Prog. Neurobiol.* **21**, 239 (1983).
38. Food (a 1-gram piece of horse meat) could be obtained on each trial by pushing open the door bearing the positive cue. The door bearing the negative cue was locked, and self-correction was not permitted. Training sessions of 40 trials occurred at the same time each day. Trials were 1 minute apart. After the end of each training session, the animals were permitted free access to food in their home cage until evening. Water was always available in the cage.
39. The day before the 2DG experiment, the cat was transported in its home cage from New York University to Brookhaven National Laboratory by car, together with the training apparatus. At the regularly scheduled time, the animal was subjected to the usual behavioral session. A dish of food was given after this test session. No further food was provided, to ensure a high level of motivation. Water was available in the cage.
40. During this period, the synthesis of the [¹⁸F]2FDG was completed after production of the requisite ¹⁸F in the cyclotron of Brookhaven National Laboratory.
41. M. Horowitz *et al.*, *Cancer Res.* **43**, 3800 (1983).
42. Note that Roman numeral refers to order in which images were obtained, not order of uptake periods.
43. Y. Yonekura *et al.*, *Science* **227**, 1494 (1985); P. Som *et al.*, *J. Nucl. Med.* **24**, 238 (1983).
44. F. Gonzalez-Lima and H. Scheich, *Neurosci. Lett.* **51**, 79 (1984).
45. The time required to cut and mount the full set of serial sections from each brain was long relative to the half-life of ¹⁸F. Thus, T1 was the actual time between placement and removal of each group of 12 sections on the sheet of film yielding the ¹⁸F ARG, and differed appreciably among images I, while T2 was essentially constant for the corresponding ¹⁴C images II.
46. A. L. Berman, *The Brain Stem of the Cat* (Univ. of Wisconsin Press, Madison, 1968).
47. The exact probability is given by $P = \sum_{i=0}^{53} C_{53}^i / 2^{53}$, see M. Woodroffe, *Probability with Applications* (McGraw-Hill, New York, 1975).
48. V. Maier and H. Scheich, *Proc. Natl. Acad. Sci. U.S.A.* **80**, 3860 (1983).
49. L. J. Porrino *et al.*, *Science* **224**, 306 (1984).
50. E. R. John, *ibid.* **177**, 850 (1972); E. R. John and E. L. Schwartz, *Annu. Rev. Psychol.* **29**, 1 (1978).
51. We thank J. Fowler for synthesis of the [¹⁸F]2DG, P. Som and D. Sacker for preparation of autoradiographs, L. Pritchard and B. Zhu for data analysis and imaging, S. John for discussions of experimental design, T. Scheitlin, H. Ahn, and C. A. Del Pin for neurosurgery and training, and M. Lobel for manuscript preparation.

2 February 1986; accepted 8 August 1986

A Yeast Gene That Is Essential for Release from Glucose Repression Encodes a Protein Kinase

JOHN L. CELENZA AND MARIAN CARLSON

The *SNF1* gene plays a central role in carbon catabolite repression in the yeast *Saccharomyces cerevisiae*, namely that *SNF1* function is required for expression of glucose-repressible genes. The nucleotide sequence of the cloned *SNF1* gene was determined, and the predicted amino acid sequence shows that *SNF1* encodes a 72,040-dalton polypeptide that has significant homology to the conserved catalytic domain of mammalian protein kinases. Specific antisera were prepared and used to identify the *SNF1* protein. The protein was shown to transfer phosphate from adenosine triphosphate to serine and threonine residues in an in vitro autophosphorylation reaction. These findings indicate that *SNF1* encodes a protein kinase and suggest that protein phosphorylation plays a critical role in regulation by carbon catabolite repression in eukaryotic cells.

CARBON CATABOLITE REPRESSION, OR GLUCOSE REPRESSION, is an important and global regulatory system in both prokaryotic and eukaryotic cells. Studies of the yeast *Saccharomyces cerevisiae* have indicated that the regulatory mechanisms effecting carbon catabolite repression in eukaryotes are different from those in bacteria, and the evidence suggests that cyclic adenosine monophosphate (AMP) is not a direct effector (1).

Genetic studies identified *SNF1* (sucrose nonfermenting) as a gene that plays a central role in carbon catabolite repression in yeast (2). The *SNF1* function is required for expression of various glucose-repressible genes in response to glucose deprivation; *snf1* mutants are unable to utilize sucrose, galactose, maltose, melibiose, or nonfermentable carbon sources, and diploids homozygous for *snf1* do not sporulate. The *snf1* mutants are not healthy strains, but are not defective in induction of acid phosphatase, an enzyme that is not regulated by glucose repression. Recent experiments (3) have shown that *SNF1* is the same gene as *CCRI*, which was independently found to be essential for derepression of several glucose-repressible enzymes (4).

The role of *SNF1* in expression of the *SUC2* (invertase) gene has been examined at the molecular level. The inability of *snf1* mutants to utilize sucrose results from a failure to derepress the *SUC2* messenger RNA encoding secreted invertase (5). Evidence that the effects of *SNF1* on *SUC2* expression occur at the transcriptional level and are mediated by the *SUC2* upstream regulatory region was obtained by showing that *SNF1* was required for expression of a heterologous yeast promoter under the control of the *SUC2* upstream regulatory region (6).

We have previously cloned the *SNF1* gene and mapped it to a locus on the right arm of chromosome IV (7). Disruption of the

J. L. Celenza and M. Carlson are in the Department of Genetics and Development and the Institute for Cancer Research, Columbia University, College of Physicians and Surgeons, New York, NY 10032.